01 Jun 2018

Formation of chromium-iron carbide by carbon diffusion in $Al_xCoCrFeNiCu$ high-entropy alloys

Mohsen Beyramali Kivy

Caitlin S. Kriewall

Mohsen Asle Zaeem
Missouri University of Science and Technology, zaeem@mst.edu

Recommended Citation

M. Beyramali Kivy et al., "Formation of chromium-iron carbide by carbon diffusion in $Al_xCoCrFeNiCu$ high-entropy alloys," *Materials Research Letters*, vol. 6, no. 6, pp. 321-326, Taylor & Francis Ltd., Jun 2018.
The definitive version is available at https://doi.org/10.1080/21663831.2018.1449767

MATER. RES. LETT., 2018
VOL. 6, NO. 6, 321–326
https://doi.org/10.1080/21663831.2018.1449767

MATERIALS RESEARCH LETTERS
Taylor & Francis
Taylor & Francis Group

ORIGINAL REPORT

Formation of chromium-iron carbide by carbon diffusion in $Al_XCoCrFeNiCu$ high-entropy alloys

Mohsen Beyramali Kivy, Caitlin S. Kriewall and Mohsen Asle Zaeem

Department of Materials Science and Engineering, Missouri University of Science and Technology, Rolla, USA

ABSTRACT

Effect of the addition of carbon on phase formations in $Al_xCoCrFeNiCu$ (x = 0.3, 1.5, 2.8) high-entropy alloys (HEAs) was studied. Free diffusion of carbon from graphite crucible resulted in the partitioning of the entire Cr from the matrix and the formation of the $(Cr,Fe)_{23}C_6$ phase in all HEAs. No other metal-carbide phase was detected. The formation of $(Cr,Fe)_{23}C_6$ enhanced the overall hardness of the HEAs. By increasing the amount of Al, the Cr amount decreased resulting in the reduction of carbon diffusion and volume fraction of the $(Cr,Fe)_{23}C_6$ phase in HEAs. The hardness of matrix phases and the overall hardness of HEAs increased with an increase in the amount of Al.

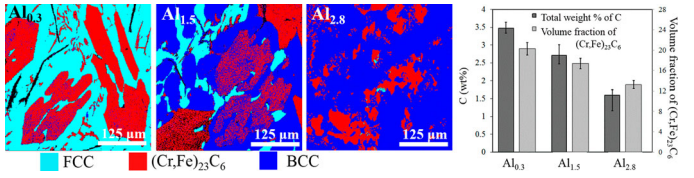

ARTICLE HISTORY
Received 19 December 2017

KEYWORDS
High-entropy alloys; carbon diffusion; carbide; $(Cr,Fe)_{23}C_6$; EBSD

IMPACT STATEMENT

The detailed phase analysis reveals that C addition to $Al_xCoCrFeNiCu$ HEAs leads to the formation of the $(Cr,Fe)_{23}C_6$ phase. The overall hardness can be controlled by the amount of C and/or Al.

Multi-principal element (MPE) alloys, also known as high-entropy alloys (HEAs), are a unique class of metallic alloys that emerged in the last two decades [1–3]. These alloys are often defined as high-disorder degree multicomponent alloys consisting of five or more alloying elements with near equi-atomic (equi-molar) compositions [2,4,5]. However, it is known that changing the compositions of the alloys can dramatically alter their microstructures [6]. Due to the high-entropy effect, most HEAs tend to form simple microstructures consisting of random solid solutions [7,8]. These alloys can be designed to have outstanding mechanical, thermal and chemical properties due to their intense lattice distortions (solution hardening), cocktail effects and sluggish atomic diffusions [2,7,9–11]. Classical design of HEAs is based on considering only substitutional alloying elements [2]. Therefore, the presence of multiple alloying elements with different atomic radii on the substitutional sites of each lattice can cause intensive lattice distortions in these alloys which can result in high mechanical strengthening [12,13]. However, it has been shown that the precipitate distribution in these alloys is sometimes challenging and can detriment the ductility of these alloys [14,15].

Recently the effect of the addition of interstitial elements to some HEAs has been investigated. In 2015, Wu et al. [16] studied the effect of the addition of interstitial carbon (C) to the equi-atomic FeNiCoCrMn alloy showing noticeable improvement in its mechanical properties, and this work started a new strategy in HEA design by doping interstitial elements. Their results showed that the addition of 0.5 at% C did not change the phase formation in the FeNiCoCrMn alloy, and the same single face-centered cubic (fcc) phase was produced with the presence of interstitial C; moreover, the addition of C enhanced both yield strength and ultimate tensile strength [16]. A similar strength improvement mechanism (interstitial strengthening) was observed in the FeNiMnAlCr alloy by doping 0.5–1 at% B or 1.1 at% C by Wang and Baker [17].

CONTACT Mohsen Asle Zaeem zaeem@mst.edu Department of Materials Science and Engineering, Missouri University of Science and Technology, 1400 N. Bishop Ave, Rolla, MO 65409, USA

In some other cases, the addition of the same interstitial elements resulted in the formation of precipitates. Li et al. studied the microstructure of $Fe_{49.5}Mn_{30}Co_{10}Cr_{10}$ (at%) HEA with the addition of 0.5 at% C [18], and their results showed the formation of nano chromium carbides causing an exceptional combination of strength and ductility for their HEA. In a different work, Laurent-Brocq et al. [19] studied the precipitation of carbonitrides in equi-molar CrMnFeCoNi HEA by adding C and N. Their results showed the formation of stable chromium carbonitrides as a result of the addition of C and N [19].

These newly designed HEAs utilize interstitial and substitutional solid solution strengthening mechanisms. However, due to the presence of multiple alloying elements in different HEA systems, phenomena such as solubility, diffusivity, and precipitation (e.g. carbide formation) need to be studied further.

In the current work, we studied the effect of free diffusion of C on phase formations in Al_xCoCrFeNiCu ($x = 0.3, 1.5, 2.8$) HEAs. Thermodynamically, the formation of aluminum carbides is favorable in such HEAs. We selected this HEA system because by increasing the amount of Al in Al_xCoCrFeNiCu HEAs the microstructure changes from single phase fcc (e.g. at $x = 0.3$) to a mixture of a dendritic body-centered cubic (bcc) and an inter-dendritic fcc (e.g. at $x = 1.5$), and then to a single phase bcc at higher amounts of Al (e.g. at $x = 2.8$) [20–22]. The inter-dendritic fcc phase (when $x = 1.5$) forms by segregation of Cu in inter-dendrite regions [23].

Investigating the effect of C diffusion in phase formations of Al_xCoCrFeNiCu HEAs is very interesting because it facilitates studying the competing mechanisms between carbide and free graphite formations in completely different microstructures created by varying the Al content. Cr plays the role of a carbide forming element, where Co and Ni are graphitizing elements which destabilize the carbides to form free graphite. It is known that the formation of chromium-carbide compounds improves the hardness and the strength of metallic alloys [24]. However, these compounds, specifically $M_{23}C_6$-type carbides, are the primary sites for fatigue crack initiations [25].

In addition to studying the effects of C on the phase formations in Al_xCoCrFeNiCu ($x = 0.3, 1.5, 2.8$) HEAs, the total amount of diffused C in the alloy systems was measured by Leco combustion analysis in this work. Diffusivity of C in crystalline materials can change based on the material structures, their packing densities, and atomic coordination [26,27]. Therefore, investigating the diffusivity of C in these HEAs, when their structures transform based on the Al content, can provide valuable information for further studies on interstitial diffusion mechanisms in these alloys. We also measured the microhardness of different phases in all three HEAs to determine the effect of the addition of C on their hardness.

To produce the HEA samples for characterization, high-purity metal powders ($>$ 99.9%; spherical gas atomized powders with the size of $\sim 40\,\mu m$) were weighed and mixed for 30 min using a Turbula mixer. The powders were then placed into an ET10 IBIDEN graphite crucible with purity of < 100 ppm ash and melted in an induction furnace (Thermal Technology LLC, Model: 1000-4560-FP30) filled with argon gas with atmospheric pressure. The samples were held at 1600°C for 1 h. After the furnace was cooled down to room temperature, the HEA samples were broken out of the graphite crucibles and sectioned. Samples were mounted in bakelite and polished using traditional metallography and polishing was sufficient to reveal the microstructures. A Nikon Ephiphot 200 optical microscope was used to observe the microstructures with visible light. A Panalytical X'Pert Pro multi-purpose diffractometer was used to perform x-ray diffraction (XRD) on HEA specimens. The XRD was scanned over 2θ angles from 5° to 100° over the period of one hour. Direct calculations as well as Panalytical Xpert Pro Software were used to index the phases in XRD patterns and the same results were obtained. Scanning electron microscopy (SEM), electron backscatter diffraction (EBSD) and energy-dispersive spectroscopy (EDS) were performed on a Helios Nanolab 600. A Tukon micro-hardness tester and a Steuers Duramin Hardness Tester were used for Vicker's hardness indentations. Each micro-hardness indentation used a 50 g load and 15 s of indentation. To determine the weight percentage of carbon that diffused into the HEA samples, a Leco CS600 was used to perform the combustion analysis.

To determine the crystallographic information such as structures and lattice constants of the formed phases in the Al_xCoCrFeNiCu HEAs with the addition of C, XRD patterns of the specimens were analyzed, as shown in Figure 1. In addition to the expected fcc and/or bcc structures as the matrix phases, an $M_{23}C_6$-type chromium-iron carbide phase was also formed in all three alloys. This phase has the Fm-3 m space group with 10.5 Å lattice constant.

In addition to the formation of the chromium-iron carbide phase, increasing the amount of Al in Al_xCoCrFeNiCu HEAs stabilizes more bcc phase with respect to the fcc phase. Furthermore, an ordered bcc phase was also observed at the highest concentration of Al ($x = 2.8$). These results are in good agreement with previous studies on Al_xCoCrFeNiCu HEAs without C [28]. According to the XRD patterns (Figure 1), the lattice parameter of the bcc structure was 2.877 Å with the Im-3m space group while it was 3.616 Å for the

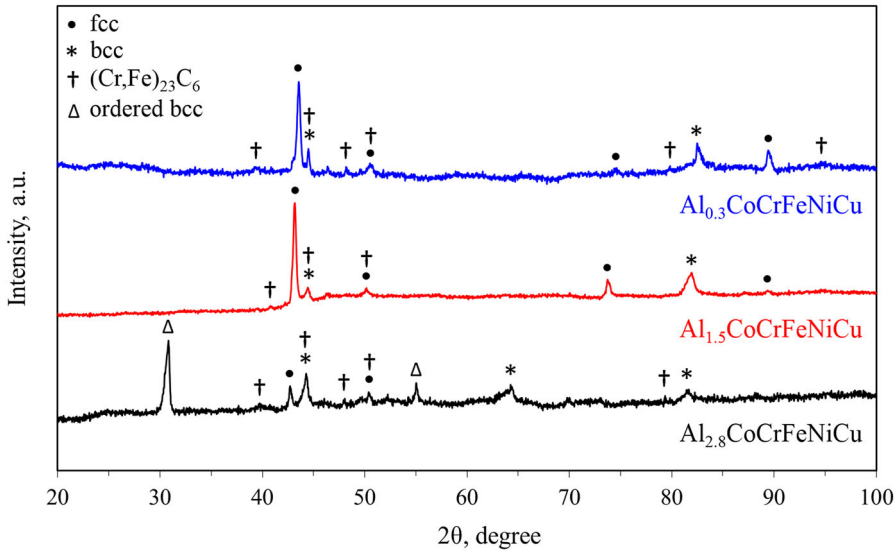

Figure 1. XRD patterns of $Al_xCoCrFeNiCu$ ($x = 0.3, 1.5, 2.8$) HEAs with the addition of C.

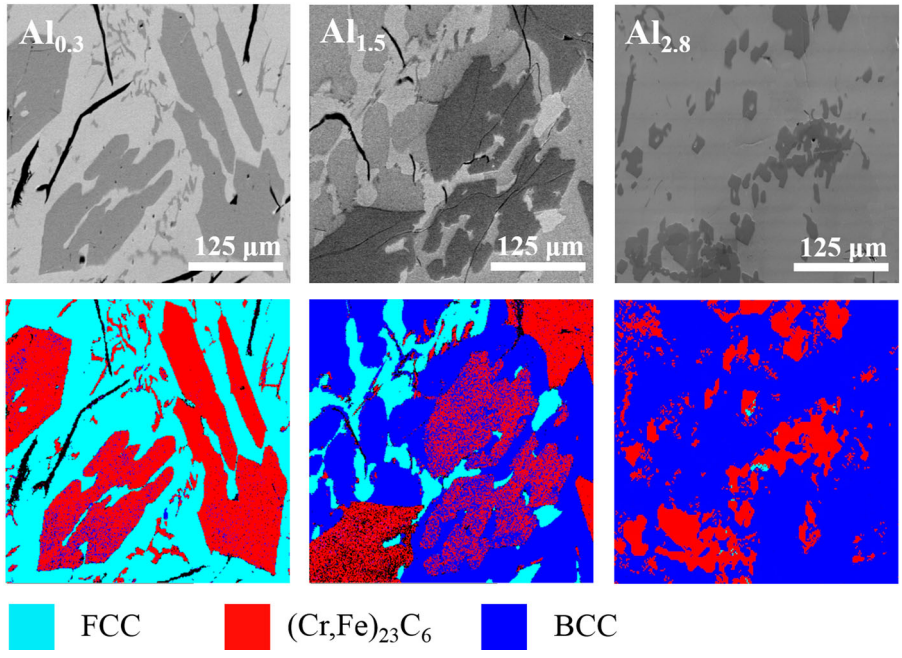

Figure 2. SEM micrographs and EBSD phase maps of (left column) $Al_{0.3}CoCrFeNiCu$, (middle column) $Al_{1.5}CoCrFeNiCu$, and (right column) $Al_{2.8}CoCrFeNiCu$. Black needle shape microstructures are graphite flakes.

fcc phase with the Fm-3 m space group. The chromium-iron carbide phase formed in HEAs was $Cr_{23-x}Fe_xC_6$ ($x = 1, 2, 3$) type. These three carbide phases have the same structures (Fm-3 m) with very similar lattice constants, $a = 10.516$ Å for $Cr_{22}FeC_6$ [29], $a = 10.507$ Å for $Cr_{21}Fe_2C_6$ [29], and $a = 10.505$ Å for $Cr_{20}Fe_3C_6$ [25]. The chromium-iron carbide phase is named $(Cr,Fe)_{23}C_6$ in the current work. It should be noted that $Cr_{22}FeC_6$ is known to be the most stable chromium-iron carbide structure due to its more negative formation and reaction energies with respect to $Cr_{21}Fe_2C_6$ and $Cr_{20}Fe_3C_6$ [25,29].

To further investigate the phases, EBSD analyses were performed on the samples. The crystallographic information obtained from XRD indexing was used to select the phases and the hit rates were 96.52%, 94.53%, and 93.79% for $Al_{0.3}CoCrFeNiCu$, $Al_{1.5}CoCrFeNiCu$, and $Al_{2.8}CoCrFeNiCu$ alloys, respectively. The EBSD phase maps (Figure 2) indicated that the addition of C caused segregation of a secondary $(Cr,Fe)_{23}C_6$ phase in all three

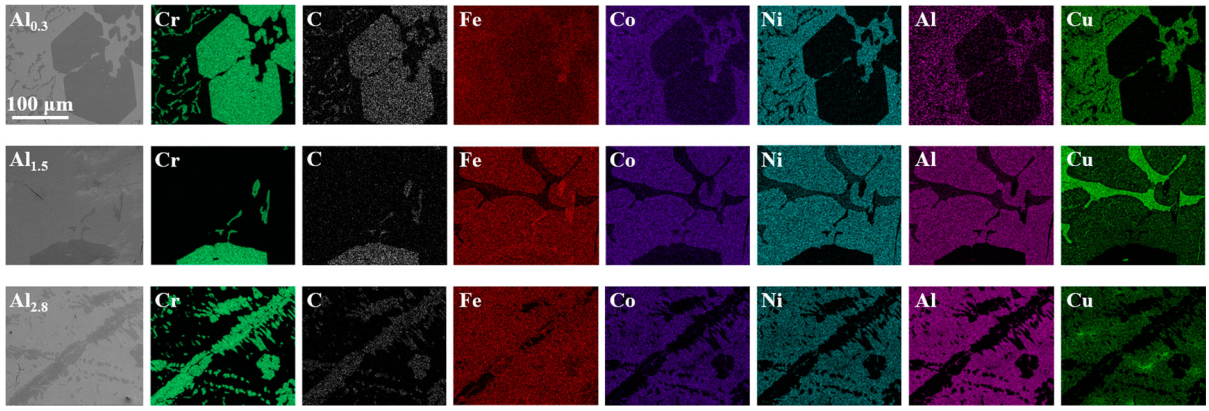

Figure 3. EDS elemental maps of (top row) $Al_{0.3}$CoCrFeNiCu, (middle row) $Al_{1.5}$CoCrFeNiCu, and (bottom row) $Al_{2.8}$CoCrFeNiCu.

HEAs. The structures of the matrix phases which were formed by the rest of the alloying elements changed from fcc ($x = 0.3$) to a mixture of fcc and bcc ($x = 1.5$) and then to a single phase bcc ($x = 2.8$) confirming the literature results on phase formations of Al_xCoCrFeNiCu without C [20–22].

The elemental EDS analyses, in Figure 3, revealed the distributions of the alloying elements in different phases observed in Figures 1 and 2. In SEM micrographs (top row in Figure 2 and left column in Figure 3), the darker regions are the $(Cr,Fe)_{23}C_6$ phase while the lighter areas are the matrix phase. As it can be seen in EDS maps (Figure 3), Fe was the only element which was presented in both carbide and matrix phases, with a lower concentration in the $(Cr,Fe)_{23}C_6$ phase and a higher concentration in the matrix phase. Cr was partitioned and formed the $(Cr,Fe)_{23}C_6$ phase with C and Fe. The matrix phase (single phase) in $Al_{0.3}$CoCrFeNiCu and $Al_{2.8}$CoCrFeNiCu HEAs contained the rest of the alloying elements. On the other hand, the EDS results for $Al_{1.5}$CoCrFeNiCu showed that the two matrix phases consisted of a Cu-rich inter-dendritic fcc phase along with a dendritic bcc phase containing Al, Co, Ni, Fe and a low amount of Cu. These results showed that the addition of C only partitioned Cr from the three studied HEAs and the rest of phases were formed similar to the cases without C [20–22].

In addition to the phase formation analyses, combustion analysis was also done for all the samples to determine the weight percentage of C that diffused into the HEA samples. The results are shown in Figure 4(a). The materials were prepared in graphite crucibles (under the exact same conditions) allowing free diffusion of C into the microstructures, however results showed different amounts of C in different samples. The amount of diffused C decreased as the molar percentage of Al increased. This shows that the diffusivity of C decreased by increasing the amount of Al.

Increasing the amount of Al is expected to stabilize the bcc structure [22]. Since the diffusion coefficient of C is generally higher in the bcc phase than in the fcc due to its lower packing density (68% in bcc, and 74% in fcc), the amount of diffused C is expected to increase by increasing the amount of Al. However, our results showed a reverse behavior. To explain this behavior, it should be noted that C partitioned Cr and formed $(Cr,Fe)_{23}C_6$ phase because the interstitial formation energies of C in Cr is lower compare to other alloying elements [30]. Therefore, increasing the molar fraction of Al, which means decreasing the molar fraction of Cr, leads to a lower diffusion of C into the HEAs. Molar fractions of Al and Cr were determined to be 0.057 and 0.19, 0.23 and 0.15, and 0.36 and 0.13, for $x = 0.3$, $x = 1.5$, and $x = 2.8$, respectively. The calculated volume fraction of the $(Cr,Fe)_{23}C_6$ phase in the HEAs (shown in Figure 4(a)) confirmed that the decreasing the amount of Cr (by increasing the amount of Al) resulted in a lower amount of diffused C. The volume fractions were calculated by the analysis of the optical micrographs using ImageJ. The phase characterization results showed that the addition of enough C can entirely partition Cr from the matrix. And even with the presence of the graphitizing elements (Co and Ni), chromium carbide could be formed if sufficient C is provided. In addition to the $(Cr,Fe)_{23}C_6$ phase, graphite flakes were also observed in the microstructures of Al_xCoCrFeNiCu HEAs. These graphite flakes had type A morphologies which are the most common graphite morphology in most iron-based alloys [31]. To analyze the amounts of graphite flakes, five different 1 mm × 1 mm areas of each sample were scanned under the optical microscope by using ImageJ, the volume fractions of graphite flakes in the micrographs were calculated. The results showed that the volume fraction of these graphite flakes decreased slightly as the Al content was increased: 11, 9, and 8 for $Al_{0.3}$, $Al_{1.5}$, and $Al_{2.8}$, respectively. This can be explained by the fact that the solubility of graphite (C) decreased by

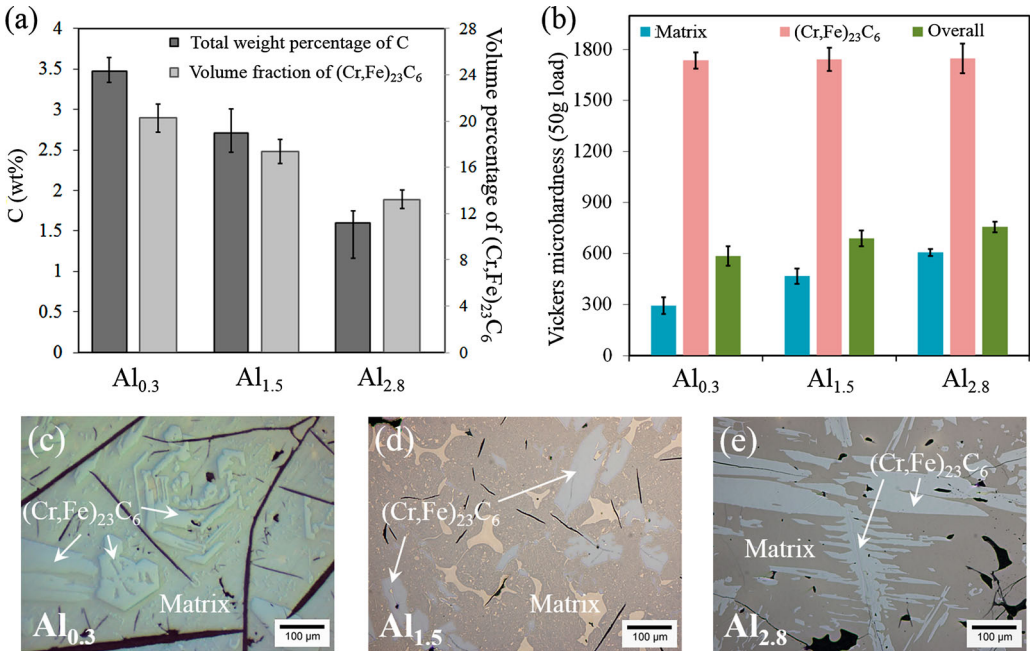

Figure 4. (a) Weight percentage of C and volume fraction of $(Cr,Fe)_{23}C_6$ phase in the microstructures of $Al_xCoCrFeNiCu$ HEAs; the error bars are standard deviations of three samples for each HEA. (b) Vickers microhardness of $Al_xCoCrFeNiCu$ HEAs; five different data points were collected for each phase of each HEA, and the error bars show the standard deviations. (c)–(e) Optical micrographs of HEAs showing the regions from which microhardness values were collected. Black needle shape microstructures in (c)–(e) are graphite flakes.

increasing the amount of Al in the alloying system [32]. These graphite flakes (black needle shape microstructures) can be seen in the micrographs of Figures 2 and 4.

Vickers microhardness of different phases of $Al_xCoCrFeNiCu$ ($x = 0.3, 1.5, 2.8$) HEAs was measured to investigate the effects of the carbon on the hardness of these HEAs and the results are illustrated in Figure 4(b). As it can be seen, the hardness of the matrix phases increased as the amount of Al increased. This trend and the hardness values are consistent with the previous reported results in the literature for $Al_xCoCrFeNiCu$ HEAs without C [20,33]. In $Al_{1.5}CoCrFeNiCu$, the hardness of the matrix is the average of both dendritic and inter-dendritic phases observed in Figure 4(d). The measured hardness of the $(Cr,Fe)_{23}C_6$ phase showed almost equivalent values in all three HEAs.

The overall microhardness of the HEAs was calculated by multiplying the microhardness of each phase by its volume fraction (Figure 4(b)). The results showed that the formation of the $(Cr,Fe)_{23}C_6$ phase enhanced the overall hardness of the HEAs. Also, the overall hardness of HEAs was increased by increasing the amount of Al. Moreover, the overall Vickers microhardness of $Al_xCoCrFeNiCu$ ($x = 0.3, 1.5, 2.8$) HEAs was measured including all the phases with or without graphite flakes. The results for all phases including graphite flakes were 365 VH, 428 VH, and 593 VH for $Al_{0.3}$, $Al_{1.5}$ and $Al_{2.8}$, respectively. And microhardness values for all phases without graphite flakes were 545 VH, 650 VH, and 756 VH for $Al_{0.3}$, $Al_{1.5}$ and $Al_{2.8}$. Since the graphite flakes are softer than other phases in the alloys, the Vickers hardness values were lower for cases including the graphite flakes compared with those without them.

In summary, the effects of the addition of C on phase formations in $Al_xCoCrFeNiCu$ ($x = 0.3, 1.5, 2.8$) HEAs were studied. The experimental characterization results showed that the free diffusion of C resulted in partitioning of entire Cr from the matrix and the formation of the high hardness $(Cr,Fe)_{23}C_6$ phase in all the HEAs. The formation of the $(Cr,Fe)_{23}C_6$ phase enhanced the overall hardness of the HEAs. The rest of elements (Al, Co, Fe, Ni and Cu) formed an fcc matrix phase in $Al_{0.3}CoCrFeNiCu$ and a bcc matrix phase in $Al_{2.8}CoCrFeNiCu$. The matrix phase in $Al_{1.5}CoCrFeNiCu$ contained a Cu-rich inter-dendritic fcc phase and a dendritic bcc phase. When the amount of Al was increased, the Cr amount was decreased; this resulted in lowering the amount of diffused C in the matrix and volume fraction of the $(Cr,Fe)_{23}C_6$ phase in HEAs. By increasing the amount of Al, the hardness of matrix phases increased due to a higher volume fraction of the bcc phase, and the overall harness of HEAs increased.

Acknowledgements

We would like to also thank Dr Joseph Newkirk and Mr Sreekar Karnati for providing high-purity powders for our

experiments, and Mr Dustin Arvola for his help in performing Leco combustion analysis.

Disclosure statement

No potential conflict of interest was reported by the authors.

Funding

The authors would like to acknowledge the funding support provided by the University of Missouri Research Board to complete this work.

ORCID

Mohsen Asle Zaeem http://orcid.org/0000-0002-5164-6122

References

[1] Senkov ON, Miller JD, Miracle DB, et al. Accelerated exploration of multi-principal element alloys with solid solution phases. Nat Commun. 2015;6:6529.
[2] Miracle D, Senkov O. A critical review of high entropy alloys and related concepts. Acta Mater. 2017;122:448–511.
[3] Zhang H, Zhong X, He Y, et al. Effect of high configuration entropy and rare earth addition on boride precipitation and mechanical properties of multi-principal-element alloys. J Mater Eng Perform. 2017;26(8):3750–3755.
[4] Kivy MB, Asle Zaeem M, Lekakh S. Investigating phase formations in cast AlFeCoNiCu high entropy alloys by combination of computational modeling and experiments. Mater Des. 2017;127:224–232.
[5] Cantor B. Multicomponent and high entropy alloys. Entropy. 2014;16(9):4749–4768.
[6] Li Z, Raabe D. Strong and ductile non-equiatomic high-entropy alloys: design, processing, microstructure, and mechanical properties. JOM. 2017;69(11):2099–2106.
[7] Kivy MB, Asle Zaeem M. Generalized stacking fault energies, ductilities, and twinnabilities of CoCrFeNi-based face-centered cubic high entropy alloys. Scr Mater. 2017;139:83–86.
[8] Ye Y, Wang Q, Lu J, et al. High-entropy alloy: challenges and prospects. Mater Today. 2016;19(6):349–362.
[9] Tsai K-Y, Tsai M-H, Yeh J-W. Sluggish diffusion in Co–Cr–Fe–Mn–Ni high-entropy alloys. Acta Mater. 2013;61(13):4887–4897.
[10] Huang S, Li W, Lu S, et al. Temperature dependent stacking fault energy of FeCrCoNiMn high entropy alloy. Scr Mater. 2015;108:44–47.
[11] Tsai M-H, Yeh J-W. High-entropy alloys: a critical review. Mate Res Lett. 2014;2(3): 1–17.
[12] Owen L, Pickering E, Playford H, et al. An assessment of the lattice strain in the CrMnFeCoNi high-entropy alloy. Acta Mater. 2017;122:11–18.
[13] Song H, Tian F, Hu Q-M, et al. Local lattice distortion in high-entropy alloys. Phys Rev Mater. 2017;1(2):023404.
[14] Salishchev G, Tikhonovsky M, Shaysultanov D, et al. Effect of Mn and V on structure and mechanical properties of high-entropy alloys based on CoCrFeNi system. J Alloys Compd. 2014;591:11–21.
[15] Senkov O, Senkova S, Woodward C. Effect of aluminum on the microstructure and properties of two refractory high-entropy alloys. Acta Mater. 2014;68:214–228.
[16] Wu Z, Parish C, Bei H. Nano-twin mediated plasticity in carbon-containing FeNiCoCrMn high entropy alloys. J Alloys Compd. 2015;647:815–822.
[17] Wang Z, Baker I. Interstitial strengthening of a fcc FeNiMnAlCr high entropy alloy. Mater Lett. 2016;180: 153–156.
[18] Li Z, Tasan CC, Springer H, et al. Interstitial atoms enable joint twinning and transformation induced plasticity in strong and ductile high-entropy alloys. Sci Rep. 2017;7:40704.
[19] Laurent-Brocq M, Sauvage X, Akhatova A, et al. Precipitation and hardness of carbonitrides in a CrMnFeCoNi high entropy alloy. Adv Eng Mater. 2017;19(5):1–4.
[20] Yeh JW, Chen SK, Lin SJ, et al. Nanostructured high-entropy alloys with multiple principal elements: novel alloy design concepts and outcomes. Adv Eng Mater. 2004;6(5):299–303.
[21] Wu J-M, Lin S-J, Yeh J-W, et al. Adhesive wear behavior of Al x CoCrCuFeNi high-entropy alloys as a function of aluminum content. Wear. 2006;261(5):513–519.
[22] Yang X, Zhang Y. Prediction of high-entropy stabilized solid-solution in multi-component alloys. Mater Chem Phys. 2012;132(2):233–238.
[23] Santodonato LJ, Zhang Y, Feygenson M, et al. Deviation from high-entropy configurations in the atomic distributions of a multi-principal-element alloy. Nat Commun. 2015;6:5964.
[24] Li Y, Gao Y, Xiao B, et al. The electronic, mechanical properties and theoretical hardness of chromium carbides by first-principles calculations. J Alloys Compd. 2011;509(17):5242–5249.
[25] Yijie Yi, Xu W, Xia F, et al. Effects of alloying elements M (M = Fe, Mo) on phase stability of $Cr_{23}C_6$ carbides from first-principles. Adv Eng Res. 2017;121:74–80.
[26] Gale WF, Totemeier TC. Smithells metals reference book. Oxford (UK): Butterworth-Heinemann; 2003.
[27] Murch GE. Diffusion in crystalline solids. Orlando (FL): Academic Press; 2012.
[28] Wang W-R, Wang W-L, Wang S-C, et al. Effects of Al addition on the microstructure and mechanical property of AlxCoCrFeNi high-entropy alloys. Intermetallics. 2012;26:44–51.
[29] Han JJ, Wang CP, Liu XJ, et al. First-principles calculation of structural, mechanical, magnetic and thermodynamic properties for γ-M 23 C 6 (M = Fe, Cr) compounds. J Phys: Condens Matter. 2012;24(50):505503.
[30] Hu X, Björkman T, Lipsanen H, et al. Solubility of boron, carbon, and nitrogen in transition metals: getting insight into trends from first-principles calculations. J Phys Chem Lett. 2015;6(16):3263–3268.
[31] Jiang H, Tan Y, Lei J, et al. Auto-analysis system for graphite morphology of grey cast iron. J Anal Methods Chem. 2003;25(4):87–92.
[32] Soiński M, Jakubus A, Kordas P, et al. The effect of aluminium on graphitization of cast iron treated with cerium mixture. Arch Foundry Eng. 2014;14(2):95–100.
[33] Jien-Wei Y. Recent progress in high entropy alloys. Ann Chim Sci Mat. 2006;31(6):633–648.